Biomedical Research (Tokyo) **40** (3) 115–123, 2019

Development of a mouse nerve-transfer model for brachial plexus injury

Hanako WAKATSUKI[1, 2], Minoru SHIBATA[2], Ken MATSUDA[2], and Noboru SATO[1]

[1] Division of Gross Anatomy and Morphogenesis, Department of Regenerative and Transplant Medicine, Niigata University Graduate School of Medical and Dental Sciences, Niigata, Japan and [2] Division of Plastic and Reconstructive Surgery, Department of Functional Neuroscience, Niigata University Graduate School of Medical and Dental Sciences, Niigata, Japan

(Received 11 March 2019; and accepted 24 April 2019)

ABSTRACT

Nerve transfer involves the use of a portion of a healthy nerve to repair an injured nerve, and the process has been used to alleviate traumatic brachial plexus injuries in humans. Study of the neural mechanisms that occur during nerve transfer, however, requires the establishment of reliable experimental models. In this study, we developed an ulnar-musculocutaneous nerve-transfer model wherein the biceps muscle of a mouse was re-innervated using a donor ulnar nerve. Similar muscle action potentials were detected in both the end-to-end suture of the transected nerve (correct-repair) group and the ulnar-musculocutaneous nerve-transfer group. Also, re-innervated acetylcholine receptor (AChR) clusters and muscle spindles were observed in both procedures. There were fewer re-innervated AChR clusters in the nerve transfer group than in the correct repair group at 4 weeks, but the numbers were equal at 24 weeks following surgery. Thus, our ulnar-musculocutaneous nerve-transfer model allowed physiological and morphological evaluation for re-innervation process in mice and revealed the delay of this process during nerve transfer procedure. This model will provide great opportunities to study regeneration, re-innervation, and functional recovery induced via nerve transfer procedures.

Injuries to peripheral nerves can cause paralysis and sensory disturbance. These injuries are often repaired by surgical reconstructive techniques since the peripheral nervous system has regenerative capability that exceeds that of the central nervous system (16). Transferring a portion of a healthy nerve to an injured nerve is referred to as nerve transfer, and is often used to treat traumatic brachial plexus injuries such as a root avulsion or any other lesion where nerve repair or nerve grafting is not applicable (8, 21). For example, Oberlin *et al.* described the partial transfer of an ulnar nerve to a biceps motor branch to restore active elbow flexion (15). Accumulating evidence suggests that this procedure results in good elbow flexion recovery with minimal deficits from ulnar nerve disturbance (7, 17, 19). Although nerve transfers have provided good clinical outcomes, the anatomical and molecular mechanisms that underlie this regenerative process remain largely unknown. Unlike simple transection and repair models in which motor neurons re-innervate the same muscle targets, nerve transfer may result in using motor neurons to innervate different muscle targets that were originally innervated by the injured motor neurons. Therefore, experimental models for nerve transfers should be developed since the regenerating mechanisms underlying the nerve transfer may be more complicated compared to the simple regeneration models.

The most popular experimental tool for studying peripheral nerve regeneration has been the rat sciatic nerve-injury model (20). Rats are preferred over

Address correspondence to: Dr. Noboru Sato
Division of Gross Anatomy and Morphogenesis, Department of Regenerative and Transplant Medicine, 1-757 Asahimachi-dori, Chuo-ku, Niigata, Niigata 951-8510, Japan
Tel: +81-25-227-2047, Fax: +81-25-227-0752
E-mail: nsato@med.niigata-u.ac.jp

mice because of their greater size, which simplifies surgical procedures. The sciatic nerve is the largest peripheral nerve, which enhances its accessibility for experimental manipulation. Recent progress in the genetic manipulation of mice, however, has made it possible to study the molecular mechanisms of peripheral nerve regeneration. Moreover, most of the peripheral nerve injuries efficiently treated by nerve transfer have occurred in the upper limbs, which makes the brachial plexus a clinically relevant model. Together, mouse brachial plexus possesses scientific validity to study nerve transfer.

In the present study, we developed an ulnar-musculocutaneous nerve-transfer mouse model that accomplished biceps re-innervation using an ulnar nerve. This model allows for assessment of the regenerative process via electromyography and morphological changes in neuromuscular junctions (NMJs) and muscle spindles in the re-innervated biceps.

MATERIALS AND METHODS

Animals. Four adult female C57BL/6J mice (8-weeks-old, 20–22 g of body weight, Japan SLC, Inc., Japan) were housed in standard cages with food and water ad libitum under a 12 hour, light/dark cycle. All procedures were approved by the Guidelines for animal experiments of Niigata University and had the approval of the ethics committee of Niigata University.

Surgical procedures. The right sides of the brachial plexus and biceps were used as an uninjured sham group. The left sides of murine axilla were subjected to the following surgical procedures. A left musculocutaneous nerve was transected simply without repair (transection: $n = 3$) (Fig. 1A). A left musculocutaneous nerve was transected and repaired using an end-to-end suture (correct repair: $n = 4$) (Fig. 1B). The proximal cut end of the left ulnar nerve was transferred to the distal cut end of the left musculocutaneous nerve (nerve transfer: $n = 4$) (Fig. 1C, E). All operations were performed at 8 weeks of age.

The mice were stabilized in a supine position after deep anesthesia with intraperitoneal injection of a mixture of 0.3 mg/kg body weight (b.w.) medetomidine, 4.0 mg/kg b.w. midazoram, and 5.0 mg/kg b.w. butorphanol (6). The left side of the brachial plexus and that of biceps were exposed via forelimb skin incision. Either a left ulnar nerve or a left musculocutaneous nerve was transected. In the nerve transfer group, to avoid contaminating the regenerated nerve via the proximal cut end of the left musculocutaneous nerve, the transected nerves were connected to the distal cut end of the left ulnar nerve (Fig. 1C, E).

Retrograde labelling of brachial plexus motor neurons and sensory neurons. The mice were anesthetized, a skin incision was performed at the forelimb, and the brachial plexus was exposed (Fig. 1D). Either an ulnar nerve or a musculocutaneous nerve was transected and 1,1'-Dioctadecyl-3,3,3',3'-tetramethylindocarbocyanine perchlorate ($DiIC_{18}(3)$; FUJIFILM Wako Pure Chemical Corporation, Japan) crystals were adhered to the nerve with a cyanoacrylate adhesive. The skin was then sutured, and the mice were euthanized one week after the surgery.

Then, the mice were transcardially perfused with 4% paraformaldehyde in 0.1 M phosphate buffered saline (PBS). The brachial plexus and the spinal cords were dissected together, and kept in the same fixatives overnight at 4°C. They were coronally sectioned into 200 μm slices using a LinearSlicer (Dosaka EM Co., Ltd., Japan), and collected in the PBS. Motor and sensory neurons of the brachial plexus were imaged using fluorescence microscopy (Axio observerA1; Zeiss, Germany).

Electromyography recording. The mice were stabilized in a supine position following deep anesthesia. The biceps muscles and innervating nerves were exposed via an upper arm skin incision. Bipolar stimulating hook electrodes (tip distance, 500 μm) made of 500 μm-diameter stainless wires (Bio Research Center, Japan) were placed proximal to the operation site of the nerve. The stimulations involved a train of 10 pulses at 2 Hz in 0.01 msec durations at 0.1 mA using a stimulus generator (Stimulus Isolator, AD Instruments Pty Ltd., Australia). For electromyography (EMG) recording, a bipolar stainless steel needle (tip distance, 1 mm) was inserted into the biceps muscles, and the reactions to stimulation were recorded on a PowerLab (AD Instruments Pty Ltd., Australia). Action potential is defined as the arithmetic mean of ten stimulations.

Immunohistology. The musculocutaneous nerve and biceps were dissected and fixed in 4% formalin overnight at 4°C, and immersed in 30% sucrose/PBS. The tissues were embedded in OCT compound (Sakura Finetek Japan Co., Ltd., Tokyo, Japan). Serial sections were cut in 30 μm thickness using a cryostat for mounting on MAS-coated slides

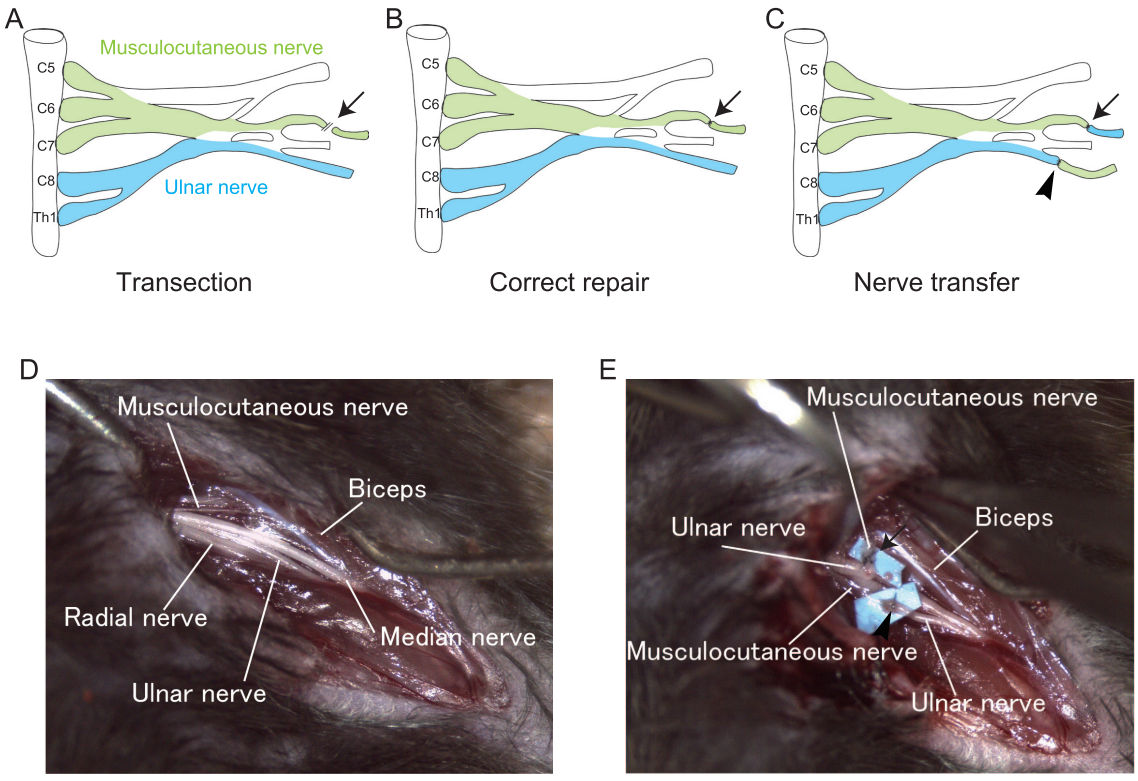

Fig. 1 Surgical procedures applied in the mouse brachial plexus. (**A**) A schematic drawing of the transection model of the musculocutaneous nerve. (**B**) A schematic drawing of the correct-repair model of the musculocutaneous nerve. (**C**) A schematic drawing of the ulnar-musculocutaneous nerve-transfer model. The donor ulnar nerve was transferred to the musculocutaneous nerve (arrow), and the musculocutaneous nerve was transferred to the ulnar nerve (arrowhead). (**D**) Frontal view of the mouse brachial plexus before surgical procedures. (**E**) Frontal view of the mouse brachial plexus after the ulnar-musculocutaneous nerve transfer. The proximal cut end of the left ulnar nerve was transferred to the distal cut end of the left musculocutaneous nerve. In addition the proximal cut end of the left musculocutaneous nerve was connected to the distal cut end of the left ulnar nerve. There were no free ends of transected nerves in this operation.

(Matsunami Glass Ind., Ltd., Kishiwada, Japan). After washing three times with 0.1 M PBS, the sections were blocked with 5% skimmed milk and 1% Triton X-100 diluted in 0.1 M PBS for 180 min at room temperature. The sections were incubated overnight with primary antibody at 4°C. A mouse monoclonal antibody for chick myosin heavy chain (S46, 1 : 6; Developmental Studies Hybridoma Bank, IA, USA) to label the muscle fibers and a rabbit antiserum for Neurofilament 200 (1 : 1000; Sigma Aldrich, Saint-Louis, MO, USA) for axon staining were used as primary antibodies. The AChRs were labeled with tetramethylrhodamine conjugated α-bungarotoxin (1 : 1000; Invitrogen, Carlsbad, CA, USA). After washing three times with PBST, the sections were incubated with secondary antibodies for one hour at room temperature. Alexa-488 of goat anti-rabbit IgG (1 : 2000, Invitrogen) or Alexa-594 of goat anti-chick IgY H&L (1 : 1000, Abcam, Cambridge, UK) were used as secondary antibodies. The sections were counterstained with 4'6-diamidino-2-phenylindole (DAPI; 1 : 10000; Sigma Aldrich) and mounted with 2.5% polyvinyl alcohol. All sections were observed using a confocal laser scanning microscope (LSM710; Zeiss, Oberkochen, Germany).

To quantify the number of AChR clusters, we checked 100 AchR clusters in each of the groups by observing every third section to avoid double counting.

RESULTS

Retrograde labelling of spinal neurons following the ulnar-musculocutaneous nerve transfer

To establish a mouse model for ulnar-musculocutaneous nerve transfer, we initially checked the anatomy of the mouse brachial plexus. Retrograde labelling of the musculocutaneous nerve showed that the musculocutaneous nerve contains motor fibers from the ventral horn of C5 to C7 and sensory fibers

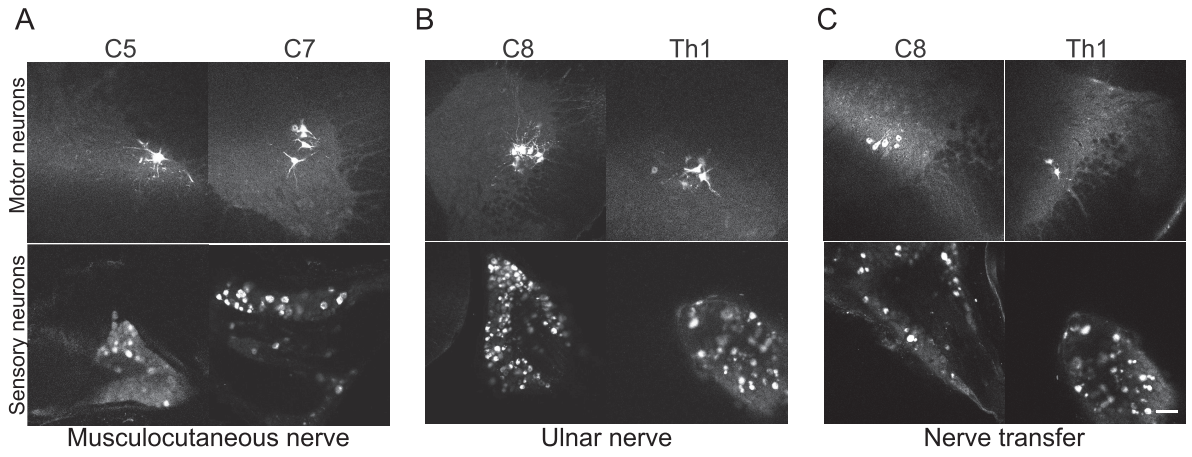

Fig. 2 Retrograde labelling of the brachial plexus nerves. (**A**) Labelling of motor and sensory neurons of the musculocutaneous nerve. The motor neurons of musculocutaneous nerves were labelled for the spinal anterior horn at the C5, C6 and C7 levels, and the sensory neurons were labelled for the DRG at the C5, C6 and C7 levels. (**B**) Motor and sensory neurons labeled for the ulnar nerve. The motor neurons of the ulnar nerve were labelled for the spinal anterior horn at the C8 and Th1 levels, and the sensory neurons of ulnar nerve were labelled for the DRG at the C8 and Th1 levels. (**C**) Motor and sensory neurons labeled after the ulnar-musculocutaneous nerve transfer. The motor and sensory neurons re-innervating the biceps were labelled at the C8 and Th1 levels of the spinal cord. Scale bar: 100 μm

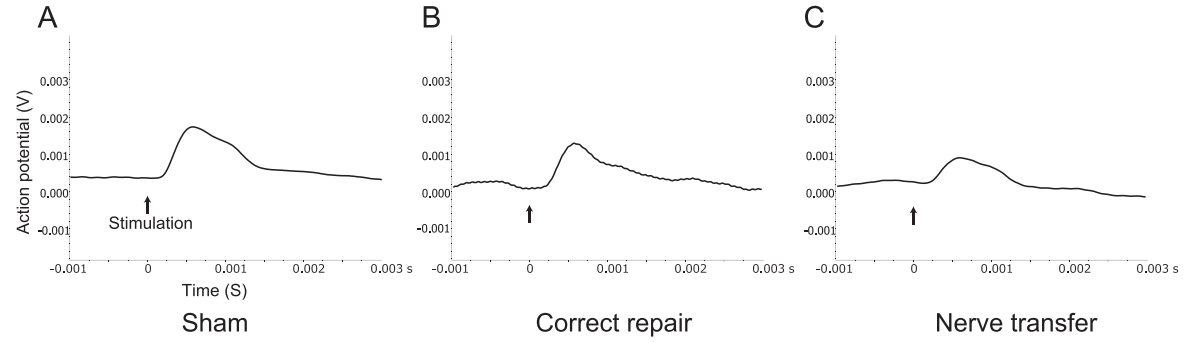

Fig. 3 Electromyography recordings of biceps at 4 weeks after nerve reconstruction. Action potential represents the arithmetic mean of 10 stimulations. The stimulations were carried out with a train of 10 pulses at 2 Hz, 0.01 m sec duration, 0.1 mA. Stimulating points are shown by arrows. (**A**) Muscle action potentials following musculocutaneous nerve stimulations of a sham model. (**B**) Muscle action potentials following stimulations at the proximal site of correct repair. (**C**) Muscle action potentials following stimulations at the proximal site of ulnar-musculocutaneous nerve transfer.

from the spinal ganglions of C5 to C7 (Fig. 2A). Conversely, the ulnar nerve originated at the C8 and Th1 levels of the cord (Fig. 2B). Thus, the motor nuclei and sensory ganglia are anatomically defined by target organs in the mouse brachial plexus.

After the ulnar-musculocutaneous nerve transfer, $DiIC_{18}(3)$ crystals were placed at a point distal to the connection site between the proximal ulnar nerve end and the distal biceps branch end, where regenerating nerve fibers could be labeled. In this case, the regenerating nerve fibers to the biceps appeared to arise from the C8 and Th1 levels of the cord, which is the origin of the ulnar nerve (Fig. 2C).

Electromyography recording

To examine the electrophysiological muscle re-innervation, the muscle action potential was recorded at 4 weeks following the surgeries. Both the correct repair and the nerve transfer showed an emergence of muscle action potential following stimulation at the proximal sites of operation (Fig. 3B, C). This result suggested that the connections between the regenerating motor nerve endings and the biceps were physiologically reconstructed in the ulnar/musculocutaneous nerve-transfer model.

Histological evaluation

Next, we checked the morphological changes at the

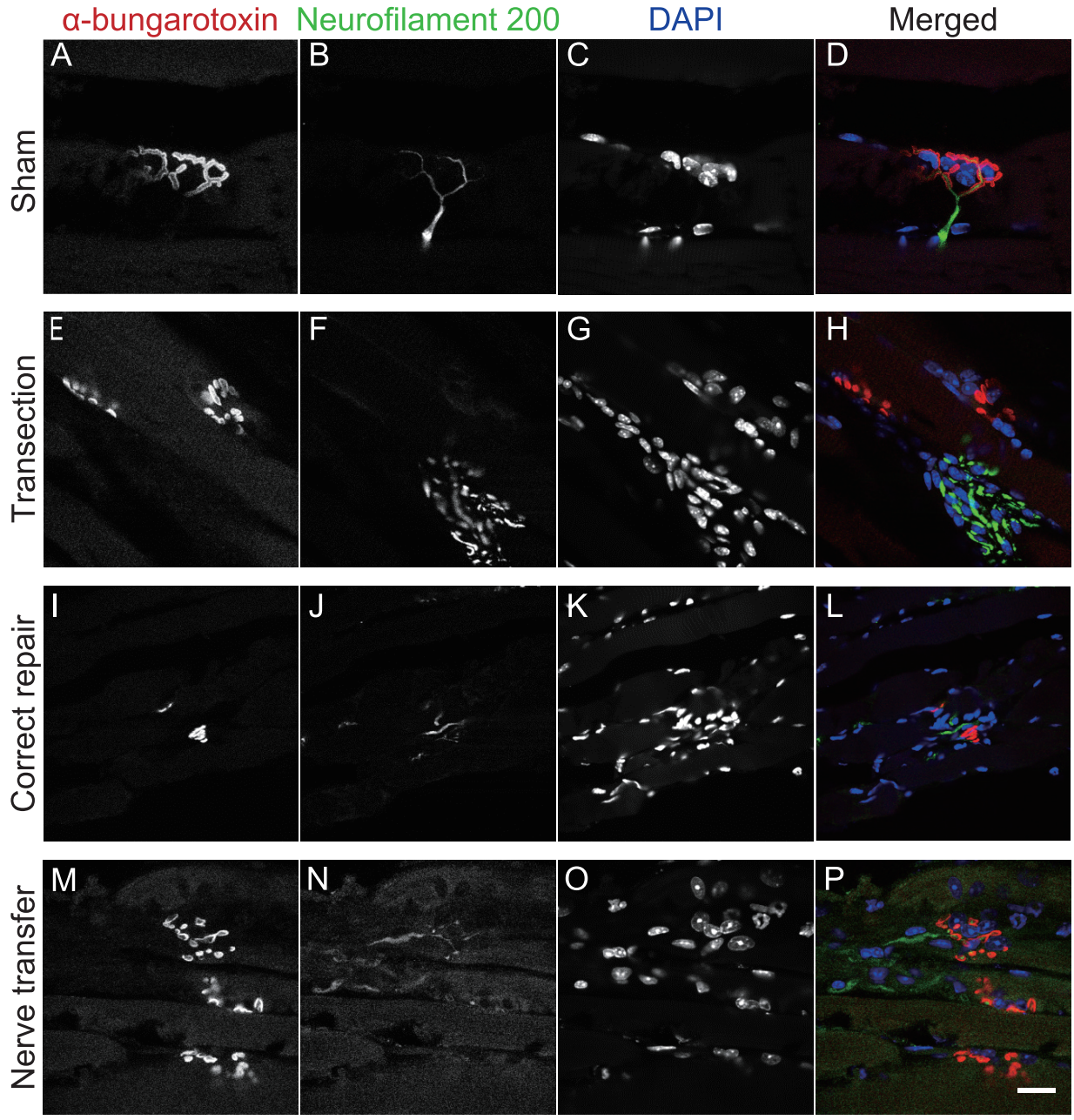

Fig. 4 Morphological analyses of the NMJs. The post synaptic AChRs were labeled with α-bungarotoxin (A, E, I, M). The axons were labeled with anti-Neurofilament 200 antibody (B, F, J, N). Cells neighboring the NMJ with nucleoli appeared to be terminal Schwann cells. (**A**–**D**) In the sham group, the motor axon occupies a junctional site, which shows a large cluster of AChRs labeled with α-bungarotoxin. (**E**–**H**) In the transected group, the axons do not occupy former synaptic sites in which clusters of AChRs become fragmented and smaller at 4 weeks after nerve resection. (**I**–**P**) In the correct-repair (I–L) and nerve-transfer (M–P) groups, the AChR clusters become fragmented and smaller as seen in the transection group. However, the regenerating axons reoccupy a part of former synaptic sites. Scale bar: 20 μm

NMJs and muscle spindles. In the sham group, the motor axons occupied the AChR clusters that had been labeled with α-bungarotoxin (Fig. 4A–D). A few annulospiral intrafusal muscle innervations were also observed at the muscle spindles (Fig. 5A–D). In the transection group, the AChR clusters had become fragmented and smaller at four weeks following the nerve resection, and these AChRs were not innervated by axons, suggesting that NMJs were not reconstructed (Fig. 4E–H). We could find no clear

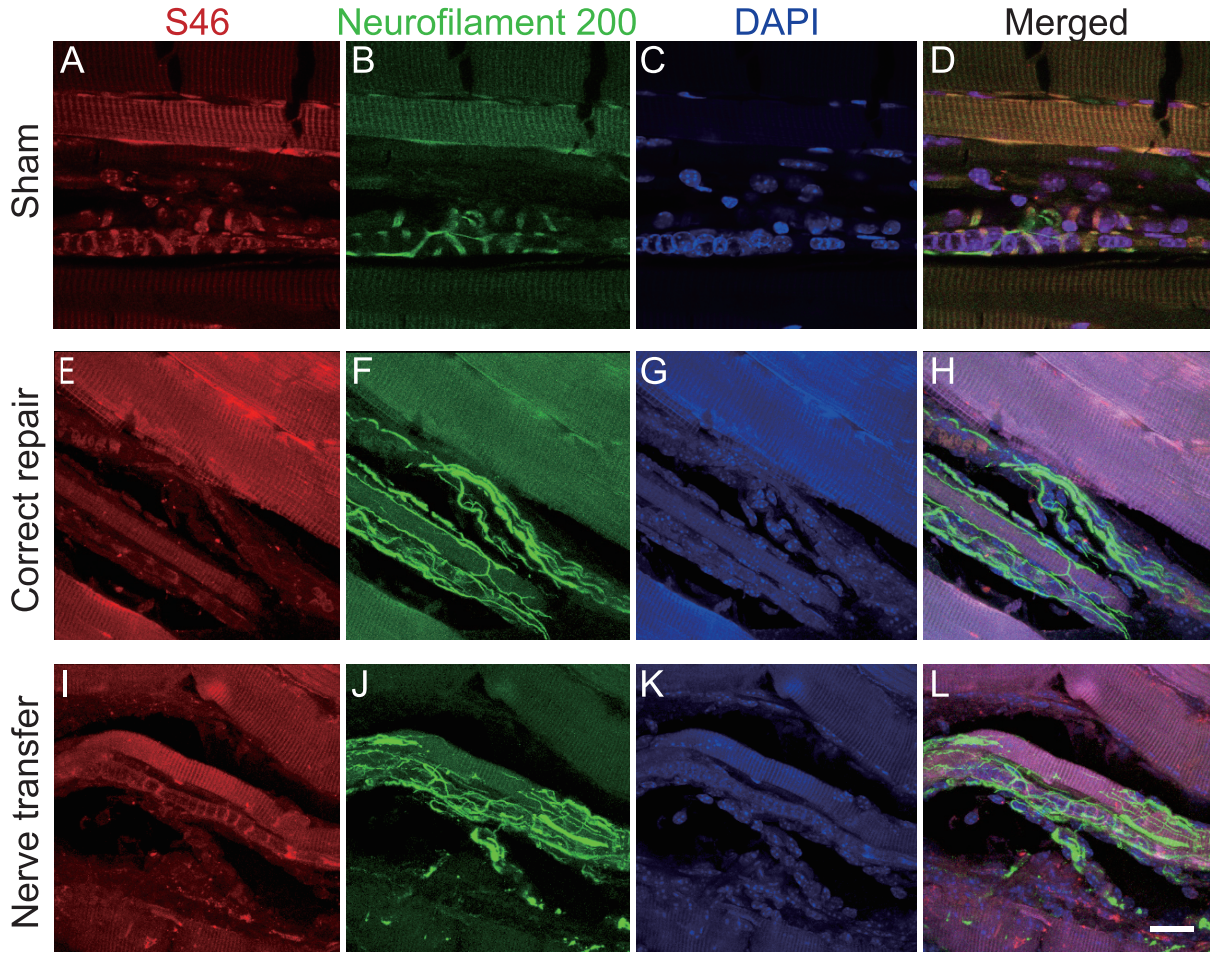

Fig. 5 Morphological analyses of the muscle spindles. Striated muscle fibers and muscle spindles of the biceps were labeled by a mouse monoclonal antibody for chick myosin heavy chain (A, E, I). The axons were labeled with anti-Neurofilament 200 antibody (B, F, J). (**A**–**D**) In the sham group, the axons were entwined with the muscle spindles in the shape of uniformed and equal interval helical structures. (**E**–**L**) In the correct-repair (E–H) and nerve-transfer (I–L) groups, the regenerating axons occupied the muscle spindles, but appeared to be deformed at four weeks following either correct repair or nerve transfer. Scale bar: 20 μm

intrafusal muscle innervation in this group. In the correct-repair and nerve-transfer groups, the AChR clusters had become fragmented and smaller, but axons occupied a portion of former synaptic sites, suggesting that a part of NMJs were at least reconstructed (Fig. 4I–P). The muscle spindles had been re-innervated, but at four weeks following either correct nerve repair or nerve transfer the nerve endings appeared irregular and distinct from a normal annulospiral structure (Fig. 5E–L). In both repair procedures, the morphological features of re-innervation were indistinguishable. Thus, the synapses, for both the NMJs and the muscle spindles, between the regenerating nerve fibers and the biceps appeared to be reconstructed in both the ulnar-musculocutaneous nerve-transfer and the normal-repair models.

Quantifying the re-innervated NMJs

We quantified the AChR clusters at 4 and 24 weeks following surgery for each of the groups. In the correct-repair group, regenerated axons occupied 72 ± 3.06 SE ($n = 4$) clusters 4 weeks after surgery, and 37 ± 2.89 SE ($n = 4$) clusters in the ulnar-musculocutaneous nerve-transfer group. At 24 weeks following surgery regenerated axons occupied 97 ± 1.73 SE ($n = 4$) clusters in the correct-repair group, and 93 ± 1.15 SE ($n = 4$) clusters in the ulnar-musculocutaneous nerve-transfer group. Therefore, while re-innervation was lessened in the ulnar-musculocutaneous nerve-transfer model at the earlier period after surgery, the longer treatment period allowed

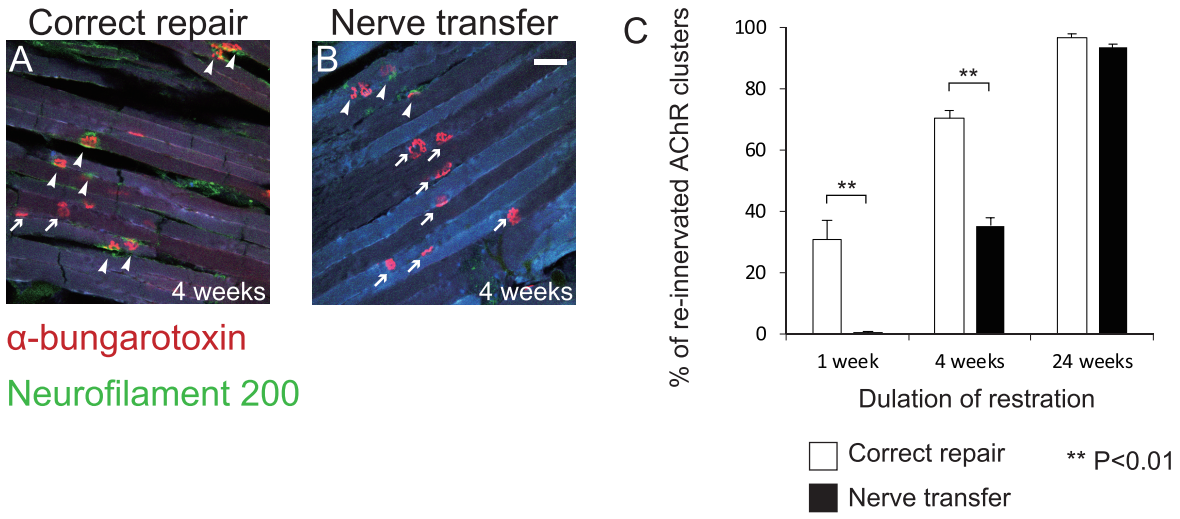

Fig. 6 Quantification of re-innervated former synaptic sites. (**A**) In the correct-repair group, regenerated axons (green: neurofilament) occupied most of sites (red: α-bungarotoxin) 4 weeks after surgery. In contrast, more than half of former synaptic sites appeared to be unoccupied by regenerated axons in the ulnar-musculocutaneous nerve-transfer (**B**) group. Re-innervated sites are shown by allowheads, while unoccupied sites are indicated by allows. Scale bar: 50 μm (**C**) The comparison of the numbers of re-innervated NMJs in correct-repair and nerve-transfer groups at 1, 4 or 24 weeks. At 1 and 4 weeks, re-innervation following the ulnar-musculocutaneous nerve transfer occurred less often compared with that following the correct-repair procedure. No differences were observed in the re-innervation ratios of both procedures at 24 weeks after surgery. Data represent the mean ± SE ($n = 4$) $^{**}P < 0.01$ for *t*-test.

re-innervation at a level that compared to that of the correct-repair model (Fig. 6).

DISCUSSION

In the present study, we focused on establishing a mouse model of nerve transfer for brachial plexus injury. We developed an ulnar-musculocutaneous nerve-transfer model and observed the process of biceps muscle re-innervation. In this model, the regenerated nerve fibers originated from the ulnar nerve at the C8 and Th1 levels of the spinal cord. Transferral of the ulnar nerve fibers re-innervated the biceps branch of the musculocutaneous nerve system, which was confirmed by detecting the muscle action potential 4 weeks following surgery. The regenerated NMJs and muscle spindles appeared similar to those observed in mice repaired via end-to-end suture of the musculocutaneous nerve, which suggests that both efferent and afferent fibers from the ulnar nerve can regenerate the synapses at a non-original muscle target.

Nerve transfers are often used in the treatment of traumatic brachial plexus injuries when root avulsion or other preganglionic injuries have occurred (12). A common example is elbow joint flexion, which is controlled by the musculocutaneous nerve. Many procedures have been described whereby donor nerves are used to restore musculocutaneous function such as the transfer of intercostal nerves (2, 10, 11, 13, 14), spinal accessory nerves (13), phrenic nerves (3), medial pectoral nerves, and fascicles from intact median and ulnar nerves (1, 15). The partial transfer of an ulnar nerve to a biceps motor branch was first described by Oberlin *et al.* (15) and is a reliable technique for the restoration of active elbow flexion (7, 17, 19). Although much clinical evidence suggests that regeneration and re-innervation have occurred via a donor nerve that had originally innervated other target muscles, the basic neural mechanisms underlying regeneration, re-innervation, and functional compensation remain largely unknown.

Neural circuit remodeling is necessary in order to restore motor function following spinal cord injury. In the periphery, in addition to motor nerve regeneration, muscle spindle feedback is known to play an important role in the recovery process (4, 18). Our model showing biceps re-innervation by both motor and sensory nerves may be very useful in studying the regenerative process of efferent and afferent fibers via the donor nerve. Moreover, the upper neural circuits might be changed to control suitable movement. Recent reports have suggested that a reorganization of the cortical circuits is induced during nerve transfer in the brachial plexus (9, 12). There-

fore, if nerve transfer can cause a reorganization of the upper neural circuits that innervate a donor nerve, corticospinal tract and ulnar nerve innervation may be modulated following ulnar-musculocutaneous nerve transfer. Moreover, the motor cortical area that controls upper limb movements and innervates the cervical segment of the spinal cord appears to be larger than expected and actually covers the area innervating the lumbar segment of the spinal cord (5). This implies that many cortical circuits are involved in upper limb movement, which gives rise to functional recovery that is supported by motor cortical plasticity following nerve transfer for brachial plexus injury.

As shown in Fig. 3, EMG recording shows no clear differences between the sham, the correct repair and the nerve transfer groups. Because an emergence of muscle action potential follows the famous all-or-non law, it cannot tell the extent of regeneration. In this study morphological analyses provided more detail features of NMJ reconstruction during the regeneration process (Figs. 4–6). Interestingly, fewer re-innervated NMJs appeared in our ulnar-musculocutaneous nerve-transfer model compared with those seen in the correct-repair model at 4 weeks following surgery. Since the number of re-innervated NMJs reached the same level for both procedures at 24 weeks, biceps re-innervation must be a longer process in ulnar-musculocutaneous nerve transfer. This may simply be due to changes in the anatomical path to the biceps muscle from the C5–C7 levels of the musculocutaneous nerve origin to the C8 and Th1 levels of the ulnar nerve origin. Moreover, brain and spinal circuit reorganization may occur, which would affect the re-innervation processes by extending the time needed for regenerating the axons to reach the AchRs under ulnar-musculocutaneous nerve-transfer conditions.

Further studies are necessary to resolve the issues mentioned above, and studies focusing on nerve-transfer models concerning upper limb movements will help define the neural mechanisms underlying re-innervation and functional recovery by a donor nerve. Our model uses a murine system that mimics Oberlin's model for human brachial plexus injury. This model in combination with the use of genetically engineered mice should help clarify the cellular and molecular mechanisms involved in nerve transfer.

In conclusion, we established an ulnar-musculocutaneous nerve-transfer model for the treatment of brachial plexus injury in mice. In this model, donor ulnar nerve regeneration and re-innervation were electrophysiologically and morphologically confirmed. This model should provide great opportunities to study regeneration, re-innervation and functional recovery induced by nerve transfer procedures, which could lead to new therapeutic methods for function recovery.

Acknowledgements

This work was supported by JSPS KAKENHI Grant Number 16K20353.

REFERENCES

1. Cho AB, Paulos RG, de Resende MR, Kiyohara LY, Sorrenti L, Wei TH, Bolliger Neto R and Mattar Junior R (2014) Median nerve fascicle transfer versus ulnar nerve fascicle transfer to the biceps motor branch in C5-C6 and C5-C7 brachial plexus injuries: nonrandomized prospective study of 23 consecutive patients. *Microsurgery* **34**, 511–515.
2. Chuang DC, Yeh MC and Wei FC (1992) Intercostal nerve transfer of the musculocutaneous nerve in avulsed brachial plexus injuries: evaluation of 66 patients. *J Hand Surg Am* **17**, 822–828.
3. Gu YD, Wu MM, Zhen YL, Zhao JA, Zhang GM, Chen DS, Yan JG and Cheng XM (1989) Phrenic nerve transfer for brachial plexus motor neurotization. *Microsurgery* **10**, 287–289.
4. Helgren ME and Goldberger ME (1993) The recovery of postural reflexes and locomotion following low thoracic hemisection in adult cats involves compensation by undamaged primary afferent pathways. *Exp Neurol* **123**, 17–34.
5. Kamiyama T, Kameda H, Murabe N, Fukuda S, Yoshioka N, Mizukami H, Ozawa K and Sakurai M (2015) Corticospinal tract development and spinal cord innervation differ between cervical and lumbar targets. *J Neurosci* **35**, 1181–1191.
6. Kirihara Y, Takechi M, Kurosaki K, Kobayashi Y and Kurosawa T (2013) Anesthetic effects of a mixture of medetomidine, midazolam and butorphanol in two strains of mice. *Exp Anim* **62**, 173–180.
7. Leechavengvongs S, Witoonchart K, Uerpairojkit C, Thuvasethakul P and Ketmalasiri W (1998) Nerve transfer to biceps muscle using a part of the ulnar nerve in brachial plexus injury (upper arm type): a report of 32 cases. *J Hand Surg Am* **23**, 711–716.
8. Mackinnon SE and Novak CB (1999) Nerve transfers. New options for reconstruction following nerve injury. *Hand Clin* **15**, 643–666, ix.
9. Maniwa K, Yamashita H, Tsukano H, Hishida R, Endo N, Shibata M and Shibuki K (2018) Tomographic optical imaging of cortical responses after crossing nerve transfer in mice. *PLoS One* **13**, e0193017.
10. Minami M and Ishii S (1987) Satisfactory elbow flexion in complete (preganglionic) brachial plexus injuries: produced by suture of third and fourth intercostal nerves to musculocutaneous nerve. *J Hand Surg Am* **12**, 1114–1118.
11. Nagano A, Ochiai N and Okinaga S (1992) Restoration of elbow flexion in root lesions of brachial plexus injuries. *J Hand Surg Am* 17, 815–821.
12. Narakas A (1978) Surgical treatment of traction injuries of the brachial plexus. *Clin Orthop Relat Res* **1978**, 71–90.
13. Narakas AO and Hentz VR (1988) Neurotization in brachial plexus injuries. Indication and results. *Clin Orthop Relat Res*

1988, 43–56.
14. Ogino T and Naito T (1995) Intercostal nerve crossing to restore elbow flexion and sensibility of the hand for a root avulsion type of brachial plexus injury. *Microsurgery* **16**, 571–577.
15. Oberlin C, Beal D, Leechavengvongs S, Salon A, Dauge MC and Sarcy JJ (1994) Nerve transfer to biceps muscle using a part of ulnar nerve for C5-C6 avulsion of the brachial plexus: anatomical study and report of four cases. *J Hand Surg Am* **19**, 232–237.
16. Ramón y Cajal S and May RM (1928) *Degeneration & Regeneration of the Nervous System*. Oxford University Press, Oxford.
17. Sungpet A, Suphachatwong C, Kawinwonggowit V and Patradul A (2000) Transfer of a single fascicle from the ulnar nerve to the biceps muscle after avulsions of upper roots of the brachial plexus. *J Hand Surg Br* **25**, 325–328.
18. Takeoka A, Vollenweider I, Courtine G and Arber S (2014) Muscle spindle feedback directs locomotor recovery and circuit reorganization after spinal cord injury. *Cell* **159**, 1626–1639.
19. Teboul F, Kakkar R, Ameur N, Beaulieu JY and Oberlin C (2004) Transfer of fascicles from the ulnar nerve to the nerve to the biceps in the treatment of upper brachial plexus palsy. *J Bone Joint Surg Am* **86-a**, 1485–1490.
20. Tos P, Ronchi G, Papalia I, Sallen V, Legagneux J, Geuna S and Giacobini-Robecchi MG (2009) Chapter 4: Methods and protocols in peripheral nerve regeneration experimental research: part I-experimental models. *Int Rev Neurobiol* **87**, 47–79.
21. Tung TH, Novak CB and Mackinnon SE (2003) Nerve transfers to the biceps and brachialis branches to improve elbow flexion strength after brachial plexus injuries. *J Neurosurg* **98**, 313–318.
22. Yamashita H, Chen S, Komagata S, Hishida R, Iwasato T, Itohara S, Yagi T, Endo N, Shibata M and Shibuki K (2012) Restoration of contralateral representation in the mouse somatosensory cortex after crossing nerve transfer. *PLoS One* **7**, e35676.